Poly(sebacic acid-*co*-ricinoleic acid) Biodegradable Injectable in Situ Gelling Polymer

Ariella Shikanov and Abraham J. Domb*

Department of Medicinal Chemistry and Natural Products, School of Pharmacy—Faculty of Medicine, The Hebrew University of Jerusalem, 91120 Jerusalem, Israel

Received September 6, 2005; Revised Manuscript Received October 26, 2005

The investigated polymers, poly(sebacic acid-*co*-ricinoleic acid) containing ≥70% ricinoleic acid, may be injected via a 22 gauge needle and become gel upon contact with aqueous medium, both in vitro and in vivo. Various properties of the polymers including viscosity, thermal analysis, and in vivo behavior, before and after exposure to aqueous medium, were determined. These polymers were observed using scanning electron microscopy (SEM) at dry and wet states. It was found that the viscosity and melting temperature of P(SA:RA) increased after exposure to buffer. The viscosity at 37 °C of P(SA:RA)3:7 had the highest increase: from 4200 cP before to 8940 cP after exposure to buffer; in the case of P(SA:RA)25:75 before exposure to buffer the viscosity was 1150 cP while after it raised to 3200 cP. The viscosity of P(SA:RA)2:8 also increased from 400 cP before exposure to buffer to 1000 cP after. On the other hand polymer without sebacic acid, (poly(ricinoleic acid)), did not show gelation properties. Thermal analysis also showed an increase in the melting point of the polymers exposed to the aqueous medium during the first 24 h of incubation. Images obtained by SEM showed formation of a three-dimensional network in polymers exposed to buffers. When injected into animals, P(SA:RA) forms a solid implant in the injection site already at 8 h postinjection.

Introduction

The objective of drug therapy is to maximize the therapeutic effect of the drug while minimizing adverse effects. Systemic delivery of drugs to localized tumors has the disadvantage of providing relatively low concentrations of the drug at proliferating cell boundaries which may be located far from the abnormal capillary networks in the tumor.[1,2] Polymer-based anticancer drug-loaded implants provide an opportunity to deliver high, localized doses of drug for a prolonged period directly into a tumor or at the site of tumor resection. Thus, development of injectable in situ setting semisolid drug depots is being studied as an alternative delivery system. These implant systems are made of biodegradable products, which can be injected via a syringe into the body and once injected, solidify to form a semisolid depot.[3] Biodegradable polyanhydrides and polyesters are useful materials for controlled drug delivery.[4−6] They have a hydrophobic backbone with hydrolytically labile anhydride and/or ester that may hydrolyze to dicarboxylic acids and hydroxy acid monomers when placed in aqueous medium. Fatty acids are suitable candidates for the preparation of biodegradable polymers, as they are natural body components, and they are hydrophobic and thus may retain an encapsulated drug for longer time periods when used as drug carriers.[7,8] Ricinoleic acid based polyanhydrides have been synthesized and used as drug carriers.[9,10] The toxicity, biodegradation, and elimination of polyanhydrides and aliphatic polyesters has been recently reviewed.[11,12] The hydrolytic degradation of aliphatic polyesters and polyanhydrides depends on various physical, chemical, and biological parameters including the hydrophobicity of monomers and polymer, crystallinity of polymer, water permeability into the polymer matrix, additives, and the degradation medium and conditions.[12] The fatty acid components of these anhydrides undergo extensive metabolism in the body and are mainly excreted in the form of carbon dioxide. The in vitro and in vivo toxicity data point to the fact that these polymers are well tolerated by the tissues and can be generally considered as biocompatible.[11]

In our previous publications, we have described the synthesis and characterization of poly(ester-anhydrides) based on sebacic acid and ricinoleic acid and their use as a biodegradable carrier for paclitaxel.[13,14] The polymers gradually degraded and released anticancer drugs for months when placed in buffer solution, while toxicity testing performed on mice indicated the safety of the polymer.[13]

Semisolid biodegradable injectable implant systems were previously[3] divided into four categories based on the mechanism of achieving solidification in vivo: (1) thermoplastic pastes, (2) in situ cross-linking systems, (3) in situ precipitation from solvent, and (4) in situ gelling organogels. Thermoplastic pastes are polymer systems, which are injected into the body as a melt and form a semisolid upon cooling to body temperature.[3] In situ cross-linked polymer networks can be formed in a variety of ways, forming solid polymer systems or gels. In situ polymer precipitation can be induced by solvent removal, a change in temperature, or a change in pH. In situ gelling organogels are composed of water-insoluble amphiphilic lipids, which swell in water and form various types of lyotropic liquid crystals.[3]

The investigated polymers, poly(sebacic acid-*co*-ricinoleic acid)3:7 and 2:8, may be injected using a regular needle (22−25 gauge) and become soft gels upon contact with aqueous medium, both in vitro and in vivo. The aim of this study was to investigate this phenomenon and to try to classify this polymer in one of the four categories mentioned above.

Materials and Methods

Materials. Ricinoleic acid (RA) 85% pure was obtained from Fluka, Buch, Switzerland and purified to 97% as determined by chromatog-

* Corresponding author. Phone: 972-2-6757573. Fax: 972-2-6757629. E-mail: adomb@md.huji.ac.il.

10.1021/bm050648+ CCC: $33.50
Published on Web 11/30/2005

Table 1. Characteristics of P(SA:RA) Used in This Study

name of polymer	M_w (Da)	M_n (Da)	ΔH (J/g)	melting point (°C)
P(SA:RA)3:7	7000	5000	15.6	37.1
P(SA:RA)25:75	7000	4200	11.4	38.6
P(SA:RA)2:8	4000	3500	6.7	38.1
PRA	3950	3575		−12.3

raphy. Sebacic acid (SA) 99% was obtained from Sigma-Aldrich (Israel). All solvents were analytical grade from BioLAB (Jerusalem, Israel) or Frutarom (Haifa, Israel) and were used without further purification. Poly (sebacic acid-*co*-ricinoleic acid), designated as p(SA:RA), was prepared as previously described.[10] Polymers having different ratios of sebacic acid and ricinoleic acid were synthesized (Table 1). The polymer structure is shown in Figure 1.

Instrumentation. Molecular weights of the poly(ester-anhydrides) were estimated on a gel permeation chromatography (GPC) system consisting of a Waters 1515 isocratic HPLC pump with a Waters 2410 refractive index (RI) detector, and a Rheodyne (Coatati, CA) injection valve with a 20-μL loop (Waters, MA). Samples were eluted with chloroform through a linear Ultrastyrogel column (Waters; 500 Å pore size) at a flow rate of 1 mL/min. The molecular weights were determined relative to those of polystyrene standards (Polyscience, Warrington, PA) with a molecular weight range of 500−20000 using a Breeze computer program.

Thermal analysis was carried out on a Mettler TA 4000-DSC differential scanning calorimeter, calibrated with Zn and In standards, at a heating rate of 10 °C/min (average sample weight of 10 mg) and on a Stuart Scientific SMP1 melting point heater. An amount of 400 mg of the polymer samples was put on the Petri dish and covered with 20 mL of buffer (0.1 M, pH 7.4). The polymer samples were prepared

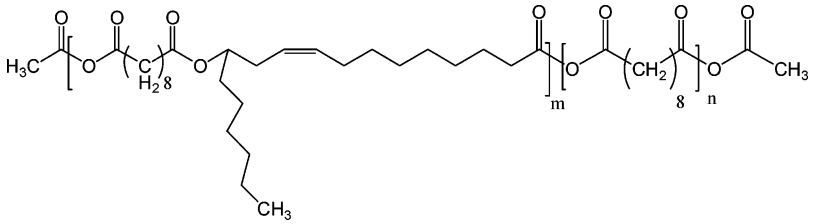

Figure 1. Structure of poly(sebacic acid-*co*-ricinoleic acid).

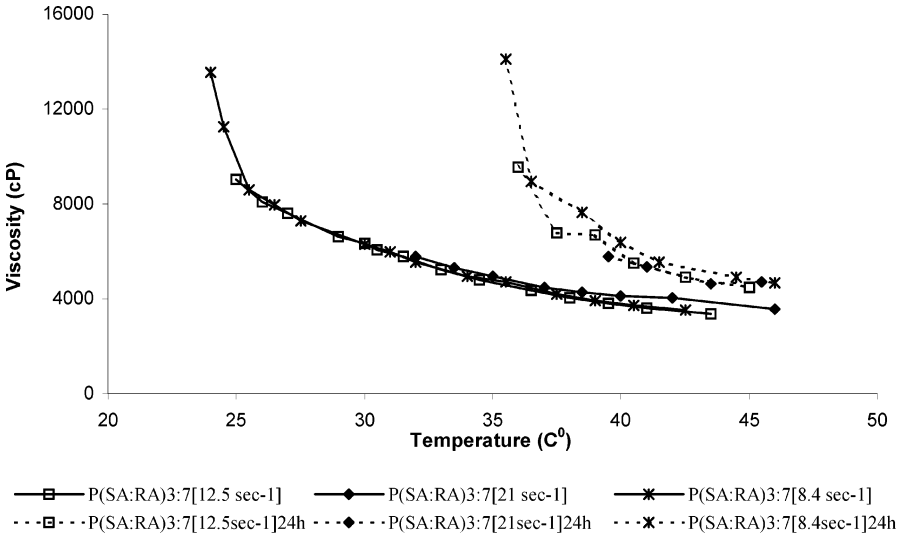

Figure 2. Viscosities of P(SA:RA)3:7 as a function of temperature at different shear rates (the shear rate applied is shown in the brackets); the solid line refers to the polymer before exposure to aqueous phase and the dashed line refers to polymer exposed to phosphate buffer, pH 7.4, 0.1 M, 37 °C for 24 h.

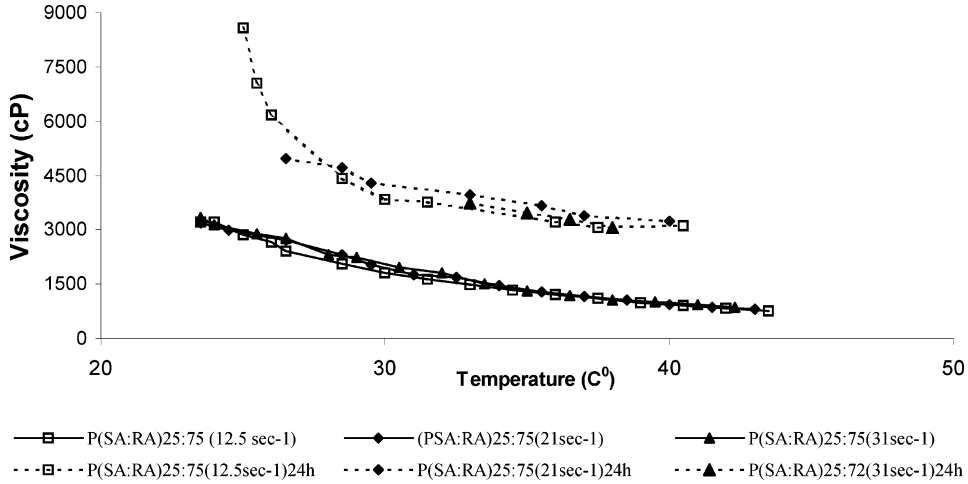

Figure 3. Viscosities of P(SA:RA)25:75 as a function of temperature at different shear rates (see Figure 2 for details).

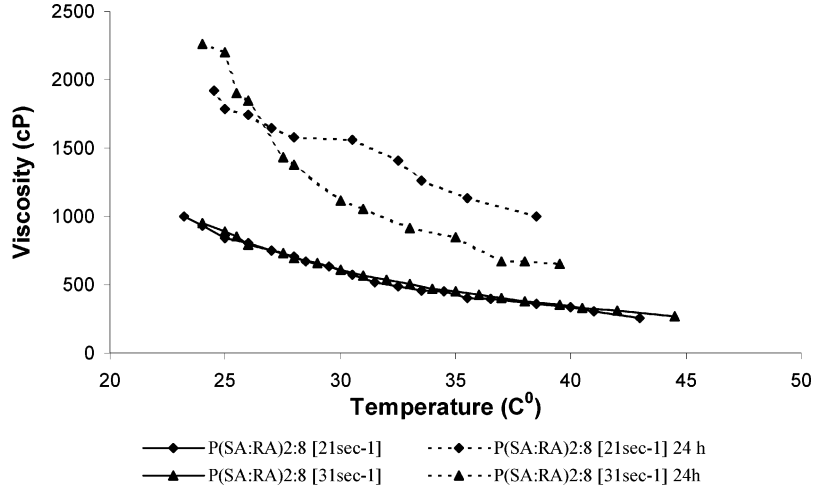

Figure 4. Viscosities of the polymer P(SA:RA)2:8 as a function of temperature at different shear rates (see Figure 2 for details).

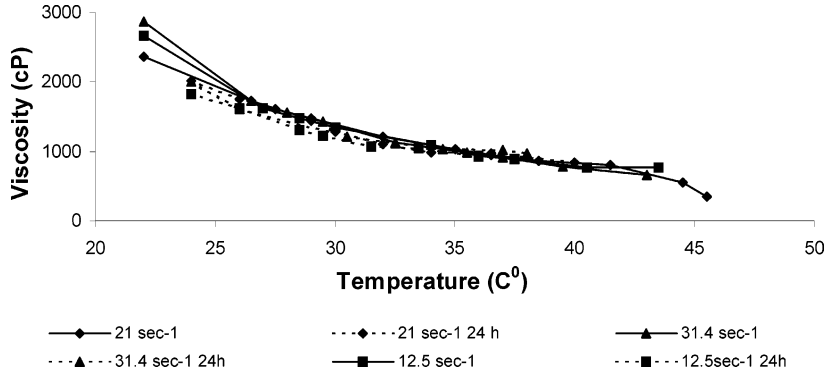

Figure 5. Viscosities of PRA as a function of temperature at different shear rates (see Figure 2 for details).

for each time point, and the experiment was prepared in triplicate. The drop of the polymer sample had dimensions of 1.5 × 1.5 × 1.5 cm^3, so at each time point when the polymer sample was pulled out of the buffer 10 mg of the sample was scratched from the surface of the drop for the outer layer analysis, and then the drop was cut 0.8 cm from the top to get the sample from the inner core of the drop.

Light Microscopy. The differences between the polymer before and after exposure to buffer were examined by microscopic observations of the samples under a stereomicroscope Stemi SV11 (Zeiss, Germany) equipped with a digital camera Cooplix 990 (Nikon, Japan) for image recording. Image recording was performed in the normal quality mode applying different microscope zoom magnifications together with the zoom of the digital camera adjusted to the best visual resolution. Illumination was performed by reflected light, supplied by a KL 1500 electronic illumination systems (Zeiss, Germany).

Cryo-scanning electron microscopy (Cryo-SEM) was conducted using a Quanta 2000 SEM (30 kV). Wet and dry polymer samples were fixed on a stub, frozen with liquid nitrogen and high vacuum, and then gold-coated using a Polarone E5100. To prepare polymer samples for Cryo-SEM the polymers were injected in buffer solution (0.1 M, pH 7.4). After 24 h the sample was pulled out and put on a stub without drying. The sample was frozen at liquid nitrogen and high vacuum. The frozen sample was gold-coated using a Polarone E5100.

Measurement of Viscosity. The viscosity of the polymer was measured using a Brookfield LVDV-III programmable viscometer coupled to a temperature-controlling unit. Cylindrical spindles were used. The polymers' viscosity was measured before the polymers were exposed to aqueous medium and after incubation for 24 h in phosphate buffer solution (0.1 M, pH 7.4) at 37 °C with constant shaking (100 rpm). To obtain a large enough sample (30 mL) to perform the viscosity measurement, 50 mL of the polymers was spread on the inner surface of a large Petri dish (2000 mL) and covered with 2000 mL of buffer. The polymer film thickness was 1−1.2 mm that was measured by caliper. After exposure to the aqueous medium the polymer sample was collected and put in the glass container. A temperature sensitivity test was performed starting at a temperature of 40 °C and down to room temperature (22 °C) by applying constant rotational speed. Detection of rheological behavior was performed by measuring the shear stress and/or viscosity at different shear rates, starting at 0.209 s^{-1}, for more viscous polymers and up to 36 s^{-1} for a less viscous polymer. All experiments were performed in triplicate.

Water Absorption. Determinations of the water content in the outer layer of the polymers stored in the phosphate buffer and in the inner core were made using Karl Fisher (KF) titration. Polymer samples (P(SA:RA)3:7 and P(SA:RA)2:8) were put in the phosphate buffer, pH 7.4, 0.1 M, 37 °C, and the KF titration was performed at 0, 4, 12, 26, and 40 h of exposure to the buffer. A separate polymer sample was prepared for each time point. At each time point, the polymer was taken out of the buffer, blotted on absorbent paper, weighed, dissolved in 1 mL of dichloromethane, and the solution was placed in the titration pot. Direct titration was performed in methanol using regular KF reagents. The sample from the inner core of the specimen was prepared similarly.

In Vivo Evaluation of Formulations. Inbred 8−10 week old female C3H mice, weighing about 20 g (Harlan Laboratories, Israel) were kept under specific pathogen-free (SPF) conditions and given free access to irradiated sterile food and acidified water throughout the experiment. Different volumes of P(SA:RA) polymers (0.05, 0.1, and 0.15 mL) were injected subcutaneously to the backspace via a 22 gauge needle. At 8 and 24 h after injection, mice were sacrificed by neck dislocation. The animal's skin was elevated, and the polymer implant was exposed and photographed. The ethics committee at the Hebrew University in Jerusalem (NIH approval number: OPRR-A01-5011) has reviewed the application for the animal study and found it compatible with the standards for care and use of laboratory animals (ethics committee research number: MD-80.04-3).

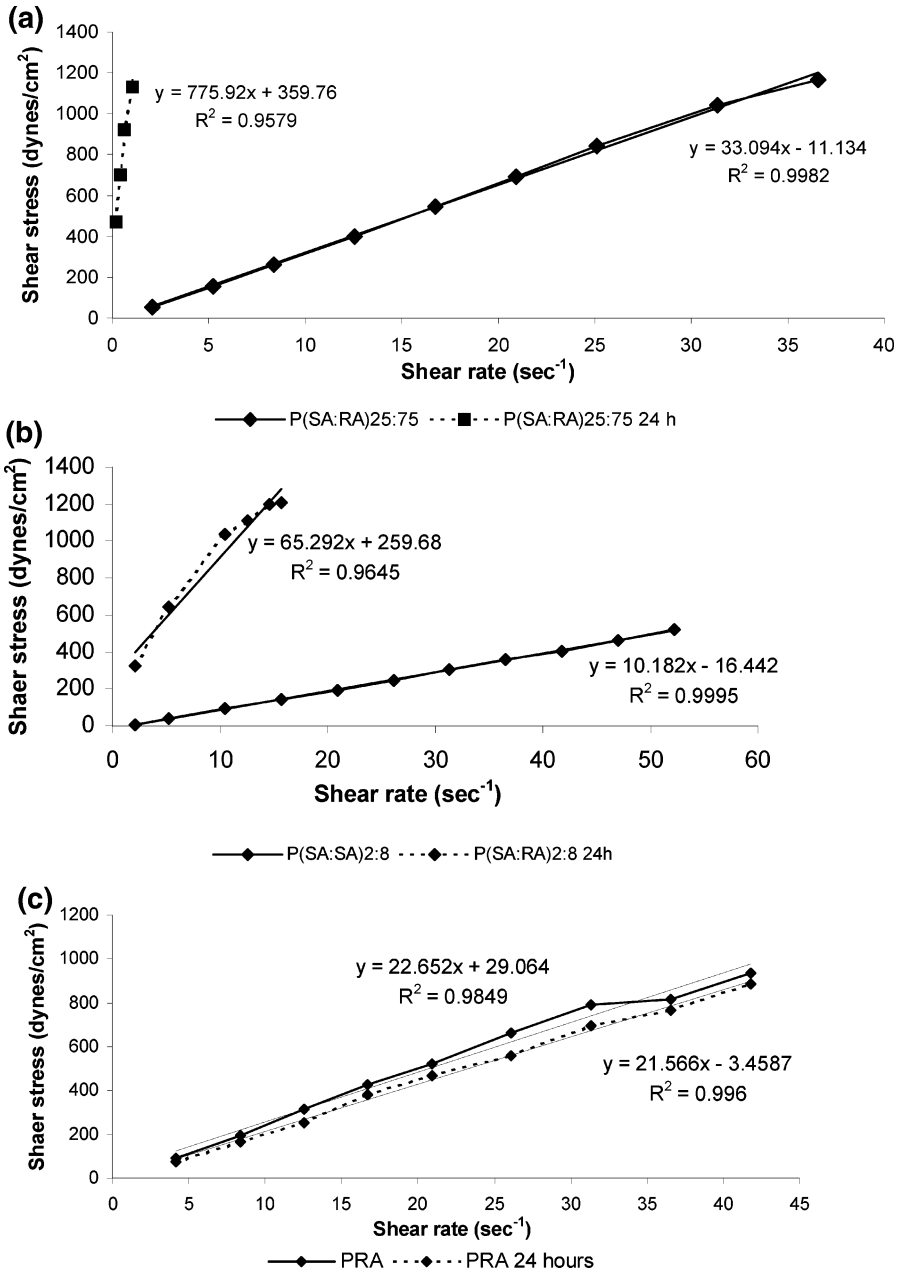

Figure 6. Relationship of shear rate/shear stress before and after exposure to aqueous medium of (a) P(SA:RA)25:75, (b) P(SA:RA)2:8, and (c) PRA. Measurements were performed at 23 °C. The viscosity before exposure to the aqueous medium is shown in the full line, and the viscosity of the polymer kept for 24 h in buffer is shown in the dashed line.

Results and Discussion

Viscosity of Polymers. One of the most obvious factors that can have an effect on the rheological behavior of a material is temperature. Some materials are quite sensitive to temperature, and a relatively small variation will result in a significant change in viscosity. Measuring viscosity at different shear rates is also important when a material is to be subjected to a variety of shear rates in processing (preparation of polymer loaded with drug by trituration) or use (injecting of the polymer via needle). Figure 2 shows the viscosities of the polymer P(SA:RA)3:7 at three different shear rates (8.4, 12.5, and 21 s^{-1}). The viscosity was measured starting at 43 °C to the lowest temperature it was possible to measure (25 °C in the case of P(SA:RA)3:7, which has the highest viscosity among the polymers described here). P(SA:RA)3:7 shows properties of a non-Newtonian fluid at lower temperatures (<30 °C), because of a nonconstant shear rate/shear stress relationship, and the polymer can be classified as a pseudoplastic shear-thinning material displaying decreasing viscosity with increasing shear rate. This behavior is important for injectability of the polymer: as pressure is applied, the polymer paste becomes softer and pumped out through the needle. At higher temperatures (>30 °C), P(SA:RA)3:7 acts as a Newtonian fluid and its viscosity is not affected by shear rate applied. The temperatures of our interest are room temperature (25 °C), because this is the temperature at which the polymer is injected, and the body temperature (37 °C), because this is the temperature to which polymer is exposed after the injection into the body. When shear rates of 8.4 s^{-1} and 12.5 s^{-1} were applied at room temperature, the viscosity of P(SA:RA)3:7 prior to exposure to aqueous medium was 8600−9000 cP, while after the exposure to water, the viscosity was too high to be measured at room temperature at those shear rates. The increase in polymer viscosity after exposure to aqueous medium at 37 °C was dependent on the shear rate: for a shear rate of 8.4 s^{-1} the

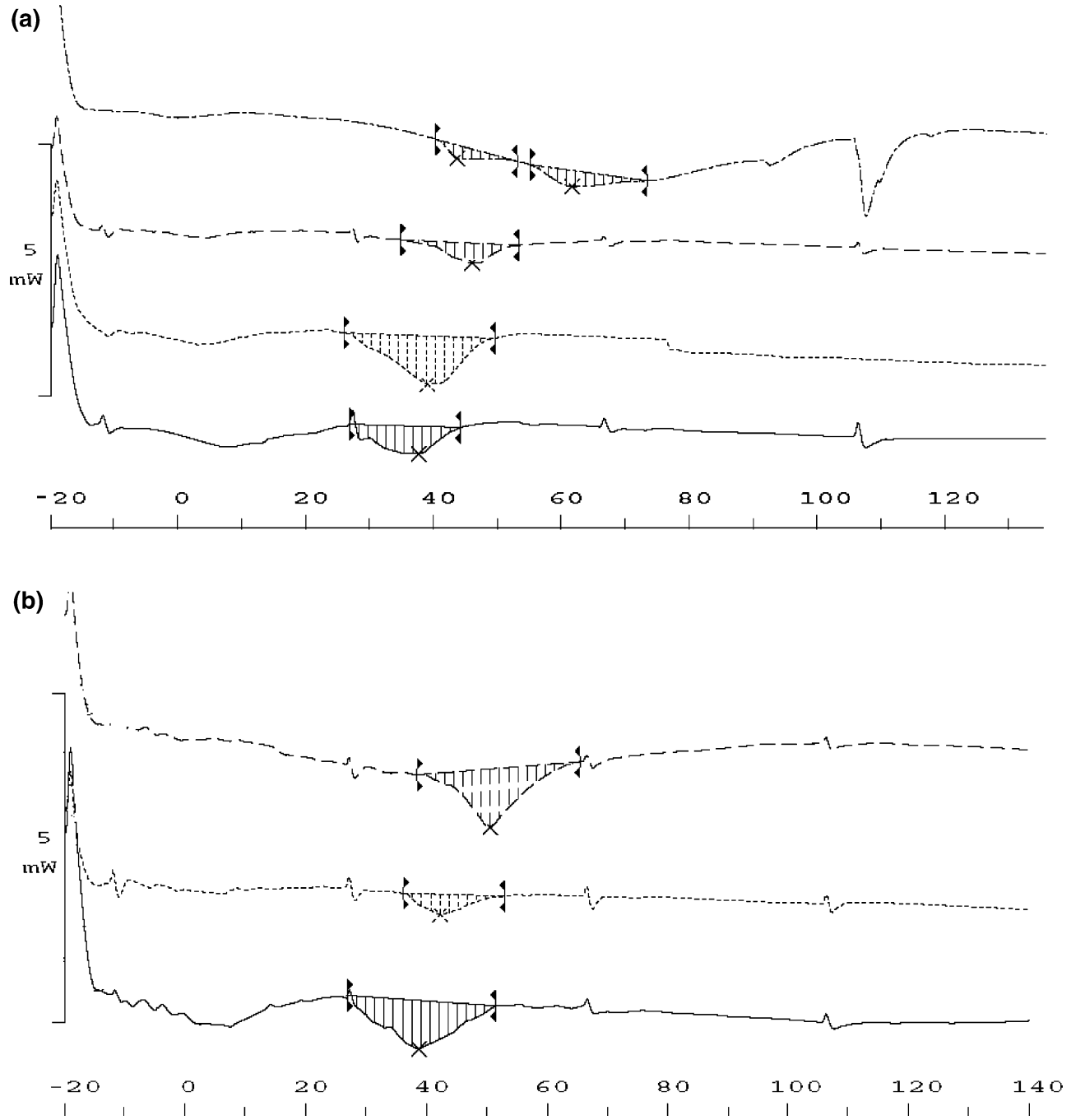

Figure 7. (a) DCS of the P(SA:RA)3:7 sample before exposure to buffer (solid line), 3 h in buffer (dotted line), 12 h in buffer (dashed line), and 24 h in buffer (dotted−dashed) line. DSC was performed on the outer layer of the polymer droplet. (b) DCS of the P(SA:RA)2:8 sample before exposure to buffer (solid line), 12 h in buffer (dashed line), and 24 h in buffer (dotted) line. DSC was performed on the outer layer of the polymer droplet.

viscosity increased from 4200 cP before to 8940 cP after exposure to buffer, at shear rate of 12.5 s^{-1} there was an increase from 4360 to 6770 cP, and at 21 s^{-1} the viscosity increased from 4115 to 5765 cP. It should be pointed out that after exposure to the aqueous medium the polymer shows a pseudoplastic behavior: this may be explained by reorganization of the polymer chains induced by the exposure to the buffer, which is destroyed at the moment of turning the spindle. The faster the rotation of the spindle (higher shear rate), the more the structure is destroyed, and the less the structure molecules slide together, the lower the viscosity will be.

Figure 3 shows the viscosities of the polymer P(SA:RA)25:75 at three different shear rates (12.5, 21, and 31 s^{-1}). The viscosity was measured starting at 43 °C to room temperature. P(SA:RA)25:75 has lower viscosity than P(SA:RA)3:7, because of its higher content of ricinoleic acid that contributes to the liquidity of the polymer. P(SA:RA)25:75 acts as a Newtonian fluid, and its viscosity is not affected by shear rate applied in this range of temperatures. Because of the polymer's lower viscosity we measured it at higher shear rates. At room temperature at all shear rates applied (12.5, 21, and 31 s^{-1}) the viscosity of P(SA:RA)25:75 prior to exposure to aqueous medium was about 2900 cP, while after the exposure viscosities were 8570 cP at 12.5 s^{-1}, 5000 cP at 21 s^{-1}, and too high to be measured at 31 s^{-1}. The viscosity of P(SA:RA)25:75 after exposure to aqueous medium when measured at 37 °C showed the behavior of a Newtonian fluid, but still there was an increase in polymer viscosity by 2200 cP (1150 cP before exposure to

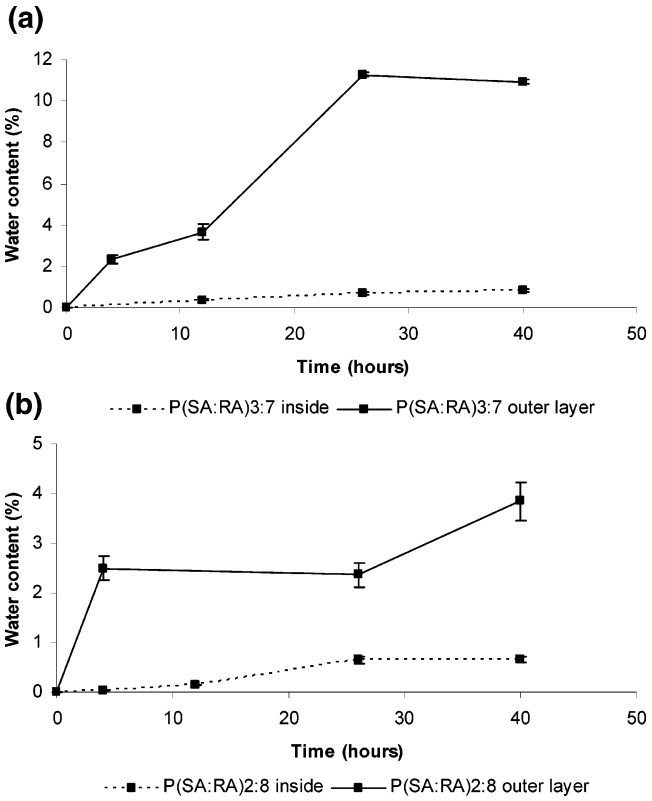

Figure 8. (a and b) Water content in P(SA:RA)3:7 and P(SA:RA)2:8 as determined by Karl Fisher titration.

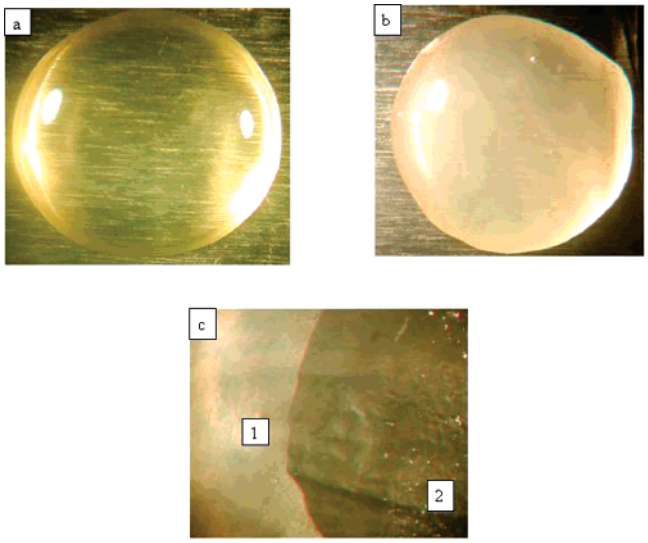

Figure 9. Light microscope pictures of (a) polymer P(SA:RA)3:7 before exposure to buffer (magnification ×10); (b) polymer P(SA:RA)3:7 after 8 h in buffer (magnification ×10); (c) cut of the polymer showing the external (exposed to buffer) side (1) and the inner core (2) (magnification ×600).

buffer and 3200 cP after). In the case of P(SA:RA)25:75 it showed pseudoplastic behavior only when the viscosity was measured at room temperature, but not at 37 °C.

Figure 4 shows the viscosities of P(SA:RA)2:8 at two different shear rates (21 and 31 s^{-1}). P(SA:RA)2:8 showed lower viscosity than that of P(SA:RA)25:75, because of its higher content of ricinoleic acid (80%). P(SA:RA)2:8 acts as a Newtonian fluid, and its viscosity is not affected by shear rate applied in this range of temperatures. Because of the polymer's lower viscosity we measured it at higher shear rates. At room temperature at both shear rates applied (21 and 31 s^{-1}) the

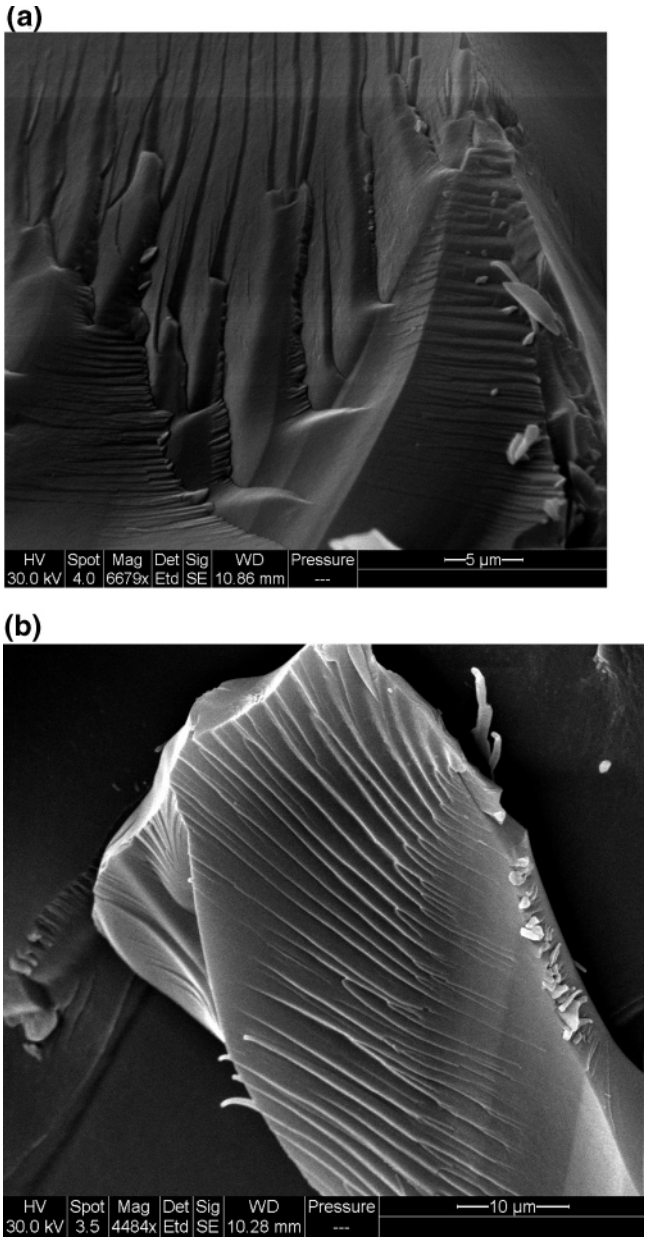

Figure 10. (a and b) SEM of the P(SA:RA)3:7 specimen before exposure to aqueous medium.

viscosity of P(SA:RA)2:8 prior to exposure to aqueous medium was about 900 cP, while after exposure, viscosities were 1800 cP at 21 s^{-1} and 1900 cP at 31 s^{-1}. The viscosity of P(SA:RA)2:8 after exposure to aqueous medium when measured at 37 °C also showed the behavior of a Newtonian fluid.

Figure 5 shows the viscosities of the polymer poly(ricinoleic acid) (PRA) at three different shear rates (12.5, 21, and 31 s^{-1}). PRA has similar viscosity to P(SA:RA)2:8, but this polymer is liquid even at 4 °C, does not change after contact with aqueous medium, and acts more like an oil. PRA acts as a Newtonian fluid, and its viscosity is not affected by shear rate applied in this range of temperatures.

The relationship between the shear stress (F) and the shear rate (dv/dr) is expressed mathematically in the Newton equation:

$$F = \eta \, dv/dr$$

where the proportionality constant, η, is the coefficient of viscosity. Parts a−c of Figure 6 show the relationship between the shear rate and shear stress of the following polymers: P(SA:

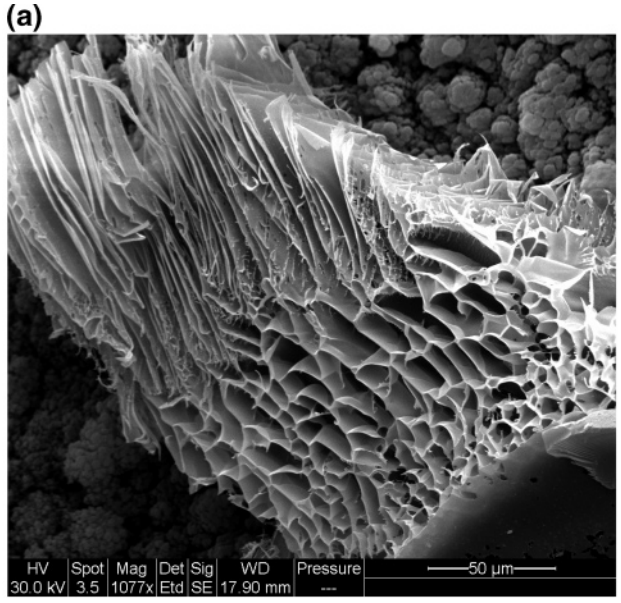

Figure 11. (a) SEM of the P(SA:RA)3:7 specimen after 24 h in aqueous phase, outer layer (1, outer layer of polymer; 2, ice surrounding sample after freezing in liquid nitrogen). (b) SEM of the P(SA:RA)3:7 (higher magnification) specimen after 24 h in aqueous phase, outer layer.

RA)25:75, P(SA:RA)2:8, and PRA before and after exposure to aqueous medium. The slope of the curve corresponding with P(SA:RA)25:75 (Figure 6a) that gelled in the aqueous medium is 23 times higher than before exposure to the aqueous phase. Figure 6b shows the relationship between the shear rate and shear stress of polymer P(SA:RA)2:8 before and after exposure to aqueous medium. The slope of the curve corresponding with P(SA:RA)2:8 that became a gel in the aqueous medium is 6.5 times higher than that before exposure to the aqueous phase. This proves that P(SA:RA)2:8 turns to a gel in the aqueous phase, although to a lesser extent than P(SA:RA)3:7 and P(SA:RA)25:75. Concerning PRA, there was no change in polymer viscosity upon exposure to aqueous medium (Figure 6c).

Differential Scanning Calorimetry. Figure 7a shows endotherms of P(SA:RA)3:7 at different durations of exposure to buffer. Before exposure of the polymer to buffer there is one transition that starts at 29.5 °C and peaks at 37.1 °C. After 3 h

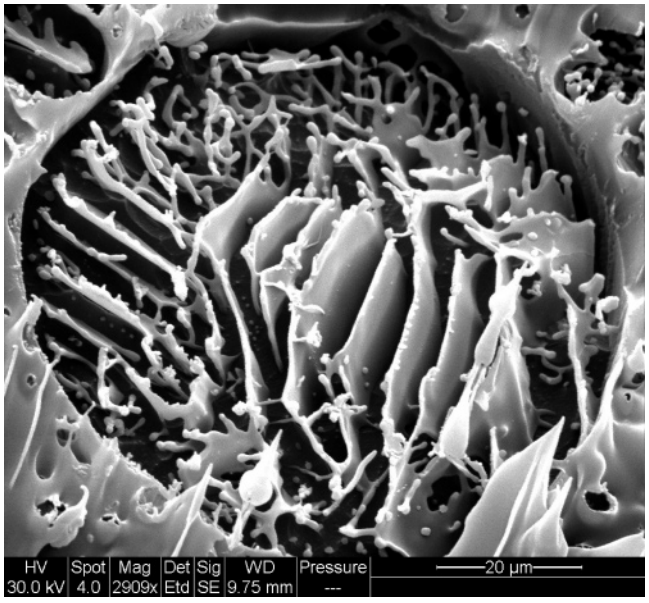

Figure 12. SEM of the P(SA:RA)3:7 specimen after 72 h in aqueous phase.

in buffer the peak was at 38.3 °C (dotted line), and at 12 h in buffer the transition became 45.5 °C. At 24 h an additional transition appeared at 61 °C that may indicate the beginning of the degradation process, i.e., a mixture of degradation products. Similar results were found for P(SA:RA)2:8 (Figure 7b). Before exposure of the polymer to buffer there is one transition that starts at a temperature of 26.7 °C and its peak at 38.1 °C. After 12 and 24 h in buffer the transition temperature became 42 °C (dotted line) and 50 °C, respectively.

Another observation made on polymers kept in the buffer is the polymer swelling capacity. It was found that P(SA:RA)2:8 and P(SA:RA)3:7 increased in their volume by 15% during first 24 h in buffer.

Water Absorption. Determination of the water content in the outer layer of the polymers stored in the phosphate buffer and in the inner core were determined using Karl Fisher titration. The results for P(SA:RA)3:7 and P(SA:RA)2:8 are summarized in Figure 8, parts a and b, respectively. The results for both polymers showed that the water content at the outer layer of the polymer that hardened upon exposure to the buffer was much higher than in the inner core of the polymer. It was found that P(SA:RA)3:7 contained 11% in the outer layer versus only 0.7% in the core after 26 h of exposure to the buffer. For P(SA:RA)2:8 the difference between the outer layer and the core was less dramatic but still significant (2.5% vs 0.6% after 26 h in the buffer).

Light Microscopy. Upon contact of the polymers with aqueous medium changes in the polymer sample are visible. These visible changes were observed using light microscopy. The polymer before exposure to buffer is transparent as shown in Figure 9a. Figure 9b shows the polymer after the gelation process took place (8 h in buffer). The polymer became opaque, and when it was cut (Figure 9c) two different regions were found: the outer region which is gel (1) and the core (2) which appears as a soft matrix.

Cryo-Scanning Electron Microscopy. Removal of the absorbed water from the exposed polymer (by drying or lyophylisation) returns it to an oily liquid with the same characteristics as before exposure to water. Cryo-microscopy allows freezing the sample while it still contains the absorbed water, and thus it was possible to visualize the polymer when

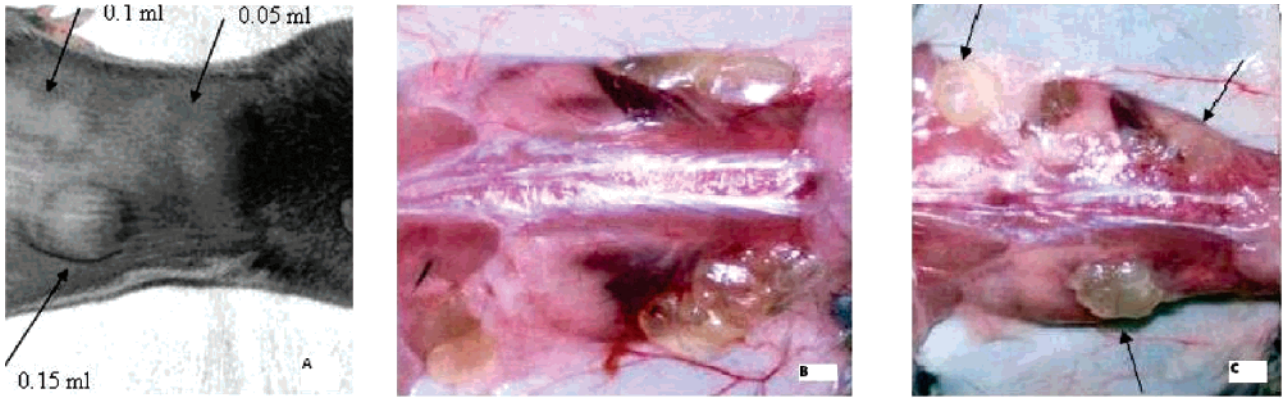

Figure 13. (A) Mouse 8 h after injection of 0.05, 0.1, and 0.15 mL of the polymer P(SA:RA)3:7 at three different places in the subcutaneous backspace. (B) Mouse sacrificed 8 h after injection of 0.05, 0.1, and 0.15 mL of the polymer P(SA:RA)3:7 at three different places in the subcutaneous backspace. (C) Mouse sacrificed 24 h after injection of 0.05, 0.1, and 0.15 mL of the polymer P(SA:RA)3:7 at three different places in the subcutaneous backspace. The injected implants are shown by arrows.

it was affected by the aqueous medium. The polymer before exposure to buffer is shown in Figure 10, parts a and b; a homogeneous surface can be seen. After the polymer sample was exposed to water (Figure 11, parts a and b) it showed a defined structure at the outer layer that was close to the aqueous medium. The polymer chains, exposed to water, build a kind of a rigid network across the drop of the polymer sample injected into the water. This network causes the polymer drop to keep its shape in the water. Figure 12 shows a surface of the polymer droplet after 72 h in buffer: there are "holes" on the polymer surface through which we see the same structure of polymer network that was observed 24 h after exposure to buffer. Cross section of the polymer droplet shows that the inside of the polymer remains intact similar to the polymer before exposure to the aqueous phase. These findings prove that gelation of the polymer occurs only on the surface that was in contact with water.

In Vivo Gelation of the Injected Formulations. Figure 13 shows mice injected with three different volumes of P(SA:RA)3:7 (0.05, 0.1, and 0.15 mL) before (Figure 13a) and after (Figure 13, parts b and c) sacrifice at 8 and 24 h, respectively. At both time points, the injected implants maintained their shape and remain in the injection site, as happens when oil is injected in the subcutaneous space. These in vivo experiments proved that polymer turned into gel in contact with tissue.

The poly(sebacic-*co*-ricinoleic acid) materials described in this study are hydrophobic polymers, built of natural fatty acids, which may be used for release of both hydrophobic and hydrophilic drugs. The purpose of this study was to investigate the gelation of these polymers upon exposure to the aqueous medium. Polymers P(SA:RA) having 70% and higher ricinoleic acid content are neither a thermoplastic or phase change paste nor an in situ cross-linked system or an in situ precipitating polymer, because there is no solvent removal and the polymer is injected as bulk.

Based on data presented in this work we can classify P(SA:RA) as an in situ forming organogel. As was defined elsewhere[15] organogels are composed of water-insoluble amphiphilic lipids, which swell in water and form various types of lyotropic liquid crystals. The nature of the liquid crystalline phase formed depends on the structural properties of the lipid, temperature, and amount of water in the system. The amphiphilic lipids examined to date for drug delivery are primarily glycerol esters of fatty acids, such as glycerol monooleate, monopalmitostearate, and monolinoleate that are waxes at room temperature. These compounds form a cubic liquid crystal phase upon injection into an aqueous medium. This liquid crystalline structure is gellike and highly viscous.[3] The P(SA:RA) materials described in this work are water-insoluble copolymers possessing viscosity and melting point increase upon exposure to aqueous medium. The rheological changes are caused by the formation of a three-dimensional network, and the image obtained using SEM showed a reversible unique physical structure that appeared upon exposure to buffer. This three-dimensional structure may be explained by hydrogen bonding between the carboxylic end groups resulting from slow hydrolytic degradation and the surrounding water molecules. A similar mechanism was suggested for lecithin bridging by hydrogen bonds in the organogel, where lipid functional groups exhibit affinity for solvents and how they bound to them.[16]

Organogels are promising injectable local delivery systems, but their limitations have been pointed out in the literature. The purity of waxes and stability of oils are the major issues that were addressed. Another drawback of organogels is the need to apply heat to mix the oil and wax phase.[3] Our polymeric system is less sensitive to the purity of polymer or solvents, and then the drug may be incorporated by trituration at room temperature without applying heat.[14]

Conclusion

We explored a gelation phenomenon of biodegradable polymers based on natural fatty acids. This process does not involve any ionic reaction or solvent removal, and the polymer is injected at room temperature. The described polymers act as organogels when exposed to aqueous medium.

Acknowledgment. This work was supported in part by a Grant dedicated to the memory of "Avra'am Ben Dov", and a Grant from Polygene. We thank the Bloom Center for Pharmaceutical Sciences at the Hebrew University for supporting in part the purchase of the scanning electron microscope.

References and Notes

(1) Brown, J. M.; Giaccia, A. J. *Cancer Res.* **1998**, *58*, 1408.
(2) Jackson, J. K.; Zhang, X. C.; Llewellen, S.; Hunter, W. L.; Burt, H. M. *Int. J. Pharm.* **2004**, *270*, 185.
(3) Hatefi, A.; Amsden, B. *J. Controlled Release* **2002**, *80*, 9.
(4) Domb, A. J. Polymers for Site Specifc Pharmacotherapy. In *Polymeric Site Specifc Pharmacotherapy*; Domb, A. J., Ed.; Wiley: Chichester, U.K., 1994; p 1.
(5) Langer, R. *Acc. Chem. Res.* **2000**, *33*, 94.
(6) Stephens, D.; Li, L.; Robinson, D.; Chen, S.; Chang, H. C.; Liu, R. M.; Tian, Y. Q.; Ginsburg, E. J.; Gao, X. Y.; Stultz, T. *J. Controlled Release* **2000**, *63*, 305.

(7) Bremer, J. *Fatty Acid Metabolism and Its Regulation*; Numa, S., Ed.; Elsevier: Amsterdam, 1984; p 113.
(8) Domb, A. J.; Rock, M.; Perkin, C.; Yipchuck, G.; Broxup, B.; Villemure, J. G. *Biomaterials* **1995**, *16*, 1069.
(9) Teomim, D.; Nyska, A.; Domb, A. J. *J. Biomed. Mater. Res.* **1999**, *45*, 258.
(10) Teomim, D.; Domb, A. J. *J. Polym. Sci., Part A: Polym. Chem.* **1999**, *37*, 3337.
(11) Katti, D. S.; Lakshmi, S.; Langer, R.; Laurencin, C. T. *Adv. Drug Delivery Rev.* **2002**, *54*, 933.
(12) Hakkarainen, M. *Degrad. Aliphatic Polyesters* **2002**, *157*, 113.
(13) Krasko, M. Y.; Shikanov, A.; Ezra, A.; Domb, A. J. *J. Polym. Sci., Part A: Polym. Chem.* **2003**, *41*, 1059.
(14) Shikanov, A.; Vaisman, B.; Krasko, M. Y.; Nyska, A.; Domb, A. J. *J. Biomed. Mater. Res., Part A* **2004**, *69A*, 47.
(15) Engstrom, S.; Engstrom, L. *Int. J. Pharm.* **1992**, *79*, 113.
(16) Shchipunov, Y. A.; Shumilina, E. V. *Mater. Sci. Eng., C* **1995**, *3*, 43.

BM050648+